Onset Transition to Cold Nuclear Matter from Lattice QCD with Heavy Quarks

M. Fromm, J. Langelage, S. Lottini, M. Neuman, and O. Philipsen

Institut für Theoretische Physik, Johann-Wolfgang-Goethe-Universität, Max-von-Laue-Strasse 1, 60438 Frankfurt am Main, Germany

(Received 17 July 2012; published 19 March 2013)

Lattice QCD at finite density suffers from a severe sign problem, which has so far prohibited simulations of the cold and dense regime. Here we study the onset of nuclear matter employing a three-dimensional effective theory derived by combined strong coupling and hopping expansions, which is valid for heavy but dynamical quarks and has a mild sign problem only. Its numerical evaluations agree between a standard Metropolis and complex Langevin algorithm, where the latter is free of the sign problem. Our continuum extrapolated data approach a first order phase transition at $\mu_B \approx m_B$ as the temperature approaches zero. An excellent description of the data is achieved by an analytic solution in the strong coupling limit.

DOI: 10.1103/PhysRevLett.110.122001 PACS numbers: 12.38.Gc, 05.70.Fh, 11.15.Ha

QCD at zero temperature is expected to exhibit the so-called silver blaze property: when a chemical potential for baryon number μ_B is switched on in the grand canonical partition function, initially all observables should be completely independent of μ_B. This changes abruptly once the chemical potential exceeds a critical value μ_{Bc}, for which the baryon number jumps from zero to a finite value and a transition to a condensed state of nuclear matter takes place. The reason for this behavior is the mass gap in the fermionic spectrum, where the nucleon mass m_B represents the lowest baryonic energy that can be populated once $\mu_B \approx m_B$. While this picture is easy to see in terms of energy levels of nucleons in a Hamiltonian language, it is elusive in the fundamental formulation of QCD thermodynamics in terms of a path integral. There, chemical potential enters through the Dirac operators of the quark fields, and hence all Dirac eigenvalues are shifted for any value of μ_B. The silver blaze property thus requires some exact cancellations for $\mu_B < m_B$.

An analytic derivation of the silver blaze property from the path integral exists only for the related case of finite isospin chemical potential $\mu_I = \mu_u = -\mu_d$ [1], where Bose-Einstein condensation of pions sets in at $\mu_I = m_\pi/2$. A numerical demonstration of the effect by means of lattice QCD has so far been impossible due to the so-called sign problem. For finite baryon chemical potential the action becomes complex, prohibiting its use in a Boltzmann factor for Monte Carlo approaches with importance sampling. Several approximate methods have been devised to circumvent this problem. These are valid in the regime $\mu \lesssim T$, where they give consistent results (for a recent review see Ref. [2]). However, the cold and dense region of QCD has so far been inaccessible to lattice simulations. A method avoiding importance sampling is stochastic quantization, where expectation values are obtained from equilibrium distributions of stochastic processes governed by a Langevin equation [3]. While this works for several models with a sign problem [4], it is not generally valid for complex actions [5]. Using Langevin dynamics, the silver blaze property has been numerically demonstrated for the Bose condensation of complex scalar fields [6]. This was recently reproduced using a worm algorithm on the flux representation of the complex action, which is free of the sign problem [7].

In this Letter we show that cold and dense lattice QCD is accessible within a 3D effective theory of Polyakov loops, which has been derived from the full lattice theory with Wilson fermions by means of strong coupling and hopping parameter expansions [8,9]. The pure gauge part reproduces the critical temperature T_c of the deconfinement transition in the continuum limit to a few percent accuracy [8]. The theory was extended to include heavy but dynamical Wilson quarks. The sign problem of the resulting effective theory being under full control, the finite-temperature deconfinement transition, including its surface of endpoints, was located for *all* chemical potentials. The critical quark mass corresponding to $\mu_B = 0$ was again found to quantitatively agree with full 4D Wilson simulations [9]. The current restriction to large quark masses ensures the validity of the hopping expansion, we comment on possible extensions later.

The lattice QCD partition function with Wilson gauge action $S_g[U]$ and $f = 1, \ldots, N_f$ quark flavors with Wilson fermion matrix $Q(\kappa_f, \mu_f)$ can be written as

$$Z = \int [dU_\mu] \prod_f \det[Q] e^{-S_g[U]} = \int [dW] e^{-S_{\rm eff}[W]};$$

$$S_{\rm eff} = S^s_{\rm eff} + S^a_{\rm eff}; \qquad S^s_{\rm eff}[W] = -\sum_{i=1}^{\infty} \lambda_i S^s_i[W];$$

$$S^a_{\rm eff}[W] = 2\sum_{f=1}^{N_f}\sum_{i=1}^{\infty}\Big[h_{if} S^a_i[W] + \bar{h}_{if} S^{a,\dagger}_i[W]\Big], \qquad (1)$$

defining a 3D effective action by integration over the spatial link variables. The $S^{s,a}_i[W]$ depend on temporal

Wilson lines $W(\mathbf{x}) = \prod_{\tau=1}^{N_\tau} U_0(\mathbf{x}, \tau)$, and the S_i^s are $Z(N_c)$ symmetric while the S_i^a are not. The couplings of the effective theory are functions of the temporal extent N_τ of the 4D lattice, the fundamental representation character coefficient $u(\beta) = \beta/18 + O(\beta^2)$ with lattice gauge coupling $\beta = 2N_c/g^2$ and the hopping parameters κ_f, which for heavy quarks are related to the quark masses as $\kappa_f = \exp(-am_f)/2$. Moreover, $\bar{h}_{if}(\mu_f) = h_{if}(-\mu_f)$. The couplings are then ordered by increasing powers of their leading contributions. Up to several nontrivial orders, the gauge sector is dominated by the nearest-neighbor interaction between Polyakov loops $L_i = \mathrm{Tr}W(\mathbf{x}_i)$,

$$e^{-S^s_{\mathrm{eff}}[W]} = \prod_{\langle ij\rangle}[1 + 2\lambda \mathrm{Re} L_i L_j^*]; \qquad (2)$$

$$\lambda(u, N_\tau \geq 5) = u^{N_\tau} \exp\Big[N_\tau\Big(4u^4 + 12u^5 - 14u^6 - 36u^7 + \frac{295}{2}u^8 + \frac{1851}{10}u^9 + \frac{1055\,797}{5120}u^{10} + \cdots\Big)\Big]. \qquad (3)$$

The convergence properties of the existing terms as well as an explicit comparison with full 4D thermal simulations demonstrate that for $\beta \lesssim 6.5$ the pure gauge sector is under control and the effect of higher couplings is negligible for $N_\tau \gtrsim 6$ [8]. When fermions are present, β is shifted by $O(\kappa^4)$ corrections, which we neglect here.

The $Z(N_c)$-breaking terms can be written as factors

$$e^{-S^a_{\mathrm{eff}}[W]} = \prod_n \Delta_n[W]. \qquad (4)$$

Summing all windings of the temporal loops this reads

$$\Delta_1 = \prod_{f,i} \det[1 + h_{1f}W_i]^2[1 + \bar{h}_{1f}W_i^\dagger]^2;$$

$$\Delta_2 = \prod_{f,\langle ij\rangle}\Big[1 - h_{2f}N_\tau \mathrm{Tr}_c \frac{W_i}{1 + C_f W_i}\mathrm{Tr}_c \frac{W_j}{1 + C_f W_j}\Big]^2, \qquad (5)$$

with the couplings

$$h_{1f} = C_f\Big[1 + 6\kappa_f^2 N_\tau \frac{u - u^{N_\tau}}{1 - u} + \cdots\Big];$$

$$h_{2f} = C_f^2 \frac{\kappa_f^2}{N_c}\Big[1 + 2\frac{u - u^{N_\tau}}{1 - u} + \cdots\Big], \qquad (6)$$

$C_f \equiv (2\kappa_f e^{a\mu_f})^{N_\tau} = e^{(\mu_f - m_f)/T}$, $\quad \bar{C}_f(\mu_f) = C_f(-\mu_f)$. From now on we consider $N_f = 1$ and drop the index "f" (i.e., $\mu = \mu_B/3$), which is sufficient to see the essential features. Finally we need meson and baryon masses,

$$am_M = -2\ln(2\kappa) - 6\kappa^2 - 24\kappa^2\frac{u}{1 - u} + \cdots,$$

$$am_B = -3\ln(2\kappa) - 18\kappa^2\frac{u}{1 - u} + \cdots. \qquad (7)$$

Let us begin our analysis of the cold and dense regime with the combined static and strong coupling limit. In this case we have $\beta = \lambda = 0$ and the partition function factorizes into exactly solvable single site integrals:

$$Z(\beta = 0) = \Big[\int dW(1 + CL + C^2L^* + C^3)^2 \times (1 + \bar{C}L^* + \bar{C}^2L + \bar{C}^3)^2\Big]^{N_s^3} = Z_1^{N_s^3}. \qquad (8)$$

The group integration only yields nonzero results if the trivial representation is contained in the products of loops. This results in the survival of hadronic degrees of freedom only,

$$\begin{aligned} Z_1 = {} & [1 + 4C^3 + C^6] + 2C[2 + 3C^3]\bar{C} \\ & + 2C^2[5 + 3C^3]\bar{C}^2 + 2[2 + 10C^3 + 2C^6]\bar{C}^3 \\ & + 2C[3 + 5C^3]\bar{C}^4 + 2C^2[3 + 2C^3]\bar{C}^5 \\ & + [1 + 4C^3 + C^6]^3\bar{C}^6 \xrightarrow{T\to 0} [1 + 4C^{N_c} + C^{2N_c}]. \end{aligned} \qquad (9)$$

We recognize the partition function of an ideal gas of baryons ($\sim C^3$), mesons ($\bar{C}C$) and composites of those, as already discussed in Ref. [10]. For finite chemical potential and zero temperature, $\bar{C} \to 0$, we are left with baryons and have reinstated N_c to illustrate the meaning of the exponents. Prefactors are identified as spin degeneracy; i.e., we have a spin-3/2 quadruplet for the three-quark baryon and a spin-zero baryon made of six quarks.

The quark density is now easily calculated,

$$n = \frac{T}{V}\frac{\partial}{\partial\mu}\ln Z = \frac{1}{a^3}\frac{4N_c C^{N_c} + 2N_c C^{2N_c}}{1 + 4C^{N_c} + C^{2N_c}}. \qquad (10)$$

In the high density limit the expression reduces to

$$\lim_{\mu\to\infty}(a^3 n) = 2N_c \equiv N_c(a^3 n_{B,\mathrm{sat}}). \qquad (11)$$

As required for fermions obeying the Pauli principle, the quark density in lattice units saturates once all available states per lattice site labeled by spin and color (and flavor for $N_f > 1$) are occupied. Note that summation over all windings of the Wilson lines is necessary in order to obtain a determinant in the form Eq. (5), while a truncation to finite order would not show saturation. Next, consider finite chemical potential and the zero temperature limit,

$$\lim_{T\to 0} a^4 f = \begin{cases} 0, & \mu < m \\ 2N_c(am - a\mu), & \mu > m \end{cases};$$

$$\lim_{T\to 0} a^3 n = \begin{cases} 0, & \mu < m \\ 2N_c, & \mu > m \end{cases}. \qquad (12)$$

Thus the static strong coupling limit shows the silver blaze property, with zero quark density for $\mu < m$ and a jump to saturation density for $\mu > m$, corresponding to a first order phase transition at quark chemical potential $\mu_c = m$. In the static strong coupling limit the baryon mass is $am_B = -3\ln(2\kappa) = 3am$; i.e., the onset happens at $\mu_B = m_B$ and satisfies the bounds in Ref. [11]. (For static quarks, $m_B/3 = m_\pi/2$). In the dense phase the free energy scales with N_c, consistent with the conjecture in Ref. [12]. For $T \neq 0$ the step function is smeared out and the transition becomes smooth, as expected for a noninteracting system.

Next we consider the interacting theory to $O(\kappa^2)$ at finite gauge coupling and quark mass. In this case the partition function has to be computed numerically and for finite values of N_τ; i.e., the zero-temperature limit has to be approached numerically. The effective theory features a sign problem, which however is mild compared to that of the full 4D theory and can be overcome by reweighting methods using a standard Metropolis algorithm. For $h_{2f} = 0$ the effective theory can be cast into a flux representation and simulated with the worm algorithm, without any sign problem. The two approaches gave consistent results for the deconfinement transition at finite temperature and density [9]. Here we include $h_2 \neq 0$, as it is the first coupling of quark-quark terms $\sim L(\mathbf{x})L(\mathbf{y})$. In this case we could not find a flux representation free of the sign problem and instead employ complex Langevin simulations as an independent check. Indeed, that algorithm has been shown to work for a simple $SU(3)$ one-site model as well as QCD in the heavy dense limit [4], which have structures very similar to our effective theory. All our simulations satisfy the convergence criterion in terms of the Langevin operator specified in Ref. [13].

In order to reach continuum QCD, we work at small parameters $\kappa \lesssim 10^{-3}$, close to but not in the static limit. In this case we can use the nonperturbative beta function of pure gauge theory for the lattice spacing in units of the Sommer parameter, $a(\beta)/r_0$ with $r_0 = 0.5$ fm [14]. Moreover, near the static limit Eq. (7) gives a good approximation to the hadron masses. Finally, temperature is tuned via $T = (aN_\tau)^{-1}$. To begin, let us consider $T =$ 10 MeV and $m_\pi = 20$ GeV. Because of the short Compton wavelength, small lattices are sufficient for baryonic quantities, with negligible differences between $N_s = 3, 6$. Once the lattice spacing is chosen, β is fixed and Eq. (7) determines the corresponding $\kappa(\beta)$.

Figure 1 shows the baryon density in lattice units as a function of chemical potential in units of the baryon mass for $\beta = 5.7$. It is consistent with zero until the chemical potential approaches $m_B/3$, where a transition or crossover is clearly visible which quickly reaches saturation level. The rise in the baryon density is accompanied by a rise in the Polyakov loop. This feature was also seen in 4D Langevin simulations [4] and in the chiral strong coupling limit in the staggered discretization [15]. By contrast, in two-color QCD with lighter masses Bose condensation and the rise of the Polyakov loop appear to reflect two distinct transitions [16]. It is not clear to us whether the rise of the Polyakov loop signals deconfinement in the presence of matter. Evaluating $\langle L^*\rangle$, $\langle L\rangle$ using Eq. (8) with $\bar{C} = 0$, the Polyakov (conjugate) loop gets screened by the third (second) terms without changing the nature of the medium,

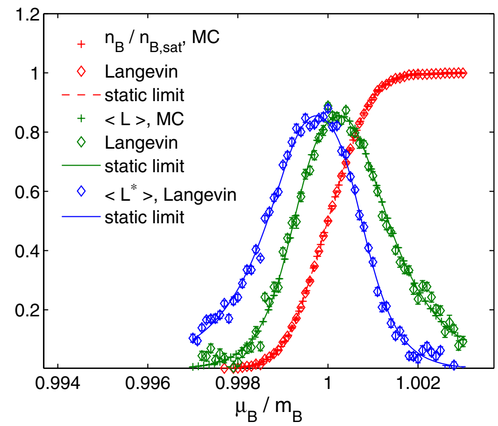

FIG. 1 (color online). Baryon density $n_B/n_{B,\mathrm{sat}}$, Polyakov loop $\langle L\rangle$ and conjugate Polyakov loop $\langle L^*\rangle$ as a function of μ_B/m_B obtained from Monte Carlo calculations ($N_s = 3$), complex Langevin ($N_s = 6$) and the static strong coupling limit, respectively. Lattice parameters $\beta = 5.7$, $\kappa = 0.0000887$, $N_\tau = 116$ correspond to $m_M = 20$ GeV, $T = 10$ MeV, $a = 0.17$ fm.

which is hadronic. This also explains why L^* is screened before L when $\mu > 0$, while the opposite happens for $\mu < 0$. The ensuing decrease is a consequence of saturation: all color orientations get populated once the lattice approaches filling. All quantities in Fig. 1 agree between the Metropolis and Langevin algorithms, the latter is vastly superior on larger volumes.

It is very striking that the numerical results are reproduced excellently by the analytic solution to the free, static hadron gas discussed earlier. That the static limit works well is easy to understand, since our quarks are exceedingly heavy and $O(\kappa^2)$ corrections are tiny. What is less obvious is that a simulation at $\beta = 5.7$ is well approximated by the strong coupling limit, $\beta = 0$. The reason is that the effective coupling of the gauge sector $\lambda(\beta = 5.7, N_\tau = 115) \sim 10^{-27}$. This is an important observation. The convergence of the strong coupling expansion is sufficiently fast to allow for an accurate estimate of the convergence radius $\beta_c < 6$ for $N_\tau \leq 16$ in Ref. [8]. For β in the same range, lowering temperature increases N_τ and thus improves convergence in two ways: we move away from the limiting convergence radius and $u(\beta) < 1$ gets suppressed by ever higher powers. In other words, cold QCD is more amenable to the strong coupling expansion than hot QCD, and the pure gauge sector plays a negligible role for the dynamics.

Simulations of the effective theory being cheap, we have computed the baryon density for nine gauge couplings $5.7 < \beta < 6.1$, corresponding to lattice spacings $0.17\ \mathrm{fm} > a > 0.07$ fm. The scaling of the result in physical units is shown in Fig. 2. Since the quark density is a derivative of the physical pressure with respect to an external parameter, it is a finite quantity that does not renormalize in a nonperturbative calculation. (The pressure requires subtraction of divergent vacuum energies,

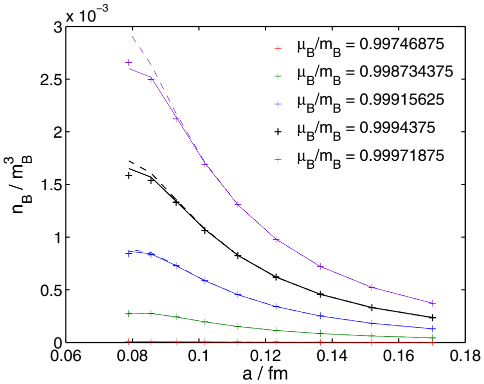

FIG. 2 (color online). Baryon density n_B/m_B^3 as a function of the lattice spacing a at $T = 10$ MeV and several values of the chemical potential. Crosses correspond to MC data ($N_s = 3$), lines to the static strong coupling limit, Eq. (5), (dashed lines) and including $\mathcal{O}(\kappa^2)$ corrections (solid lines).

$p_{\text{phys}}(T) = p(T) - p(0)$; however, these are μ independent and $\partial_\mu p_{\text{phys}}$ is finite.) Massive Wilson fermions have $O(a)$ lattice corrections; hence, the continuum approach is

$$\frac{n_{B,\text{lat}}(\mu)}{m_B^3} = \frac{n_{B,\text{cont}}(\mu)}{m_B^3} + A(\mu)a + B(\mu)a^2 + \cdots \quad (13)$$

This behavior is borne out by the data for $a > 0.09$ fm in Fig. 2. On the other hand, for $a \to 0$ we see a downward bend that violates scaling and signals that our truncated series in β, κ are no longer valid: as the lattice gets finer, β and $\kappa(\beta)$ grow and our effective action eventually must fail. Adding or removing $O(\kappa^2)$ corrections indeed affects this downward bend, but not the rest of the curve. Note that there is a trade-off between κ and β. The lighter we make the quark mass, the larger κ for a given lattice spacing and the earlier the breakdown of the hopping expansion. Thus the scaling behavior of the baryon density tells us when our effective theory breaks down.

For the very heavy quarks studied here, our series are controlled for lattice spacings down to $a \gtrsim 0.09$ fm, which is just entering the regime with leading order lattice corrections. Cutting our data for $a < 0.09$–0.11 fm, we perform continuum extrapolations based on five to seven lattice spacings by fitting to Eq. (13). We have followed this procedure for four different temperatures, resulting in the baryon densities in Fig. 3. Clearly, the silver blaze property and a jump in baryon density get realized also in the interacting, dynamical theory as the temperature approaches zero. Interestingly, the saturation density beyond onset, when expressed in units of m_B, is of the same order of magnitude as the physical nuclear density $\sim 0.16\ \text{fm}^{-3} \approx 0.15 \times 10^{-2}\ m_{\text{proton}}^3$. Finite size analyses using $N_s = 3,\ 4,\ 6,\ 8$ show that the onset at $T = 2.5$ MeV is still a smooth crossover; i.e., T is too high for a first order transition. Presently T cannot be drastically

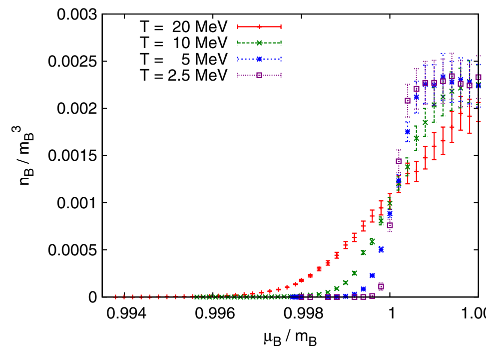

FIG. 3 (color online). Baryon density in the continuum. In the zero temperature limit a jump to nuclear matter builds up.

reduced because κ^2 corrections to the determinant get enhanced $\sim N_\tau$, Eq. (5). For physical quark masses the onset transition persists up to $T \sim 10$ MeV. More work is needed to study whether this difference is due to the larger quark mass or to the truncation of the hopping series.

For light quarks, our truncated hopping series is not reliable. How far the series can be extended and whether the pure gauge sector is similarly suppressed remains to be seen. We plan to address κ^4 corrections and details of the Langevin simulations in a future publication.

This project is supported by the German BMBF, Contract No. 06MS9150 and by the Helmholtz International Center for FAIR within the LOEWE program launched by the State of Hesse.

[1] T. D. Cohen, Phys. Rev. Lett. **91**, 222001 (2003).
[2] O. Philipsen, Acta Phys. Pol. B Proc. Suppl. **5**, 825 (2012).
[3] G. Parisi and Y.-S. Wu, Scientia Sinica **24**, 483 (1981).
[4] G. Aarts and I.-O. Stamatescu, J. High Energy Phys. 09 (2008), 018.
[5] P. H. Damgaard and H. Hüffel, Phys. Rep. **152**, 227 (1987).
[6] G. Aarts, Phys. Rev. Lett. **102**, 131601 (2009).
[7] C. Gattringer and T. Kloiber, Nucl. Phys. **B869**, 56 (2013).
[8] J. Langelage, S. Lottini, and O. Philipsen, J. High Energy Phys. 02 (2011), 057; 07 (2011), 014(E).
[9] M. Fromm, J. Langelage, S. Lottini, and O. Philipsen, J. High Energy Phys. 01 (2012), 042.
[10] J. Langelage and O. Philipsen, J. High Energy Phys. 04 (2010), 055.
[11] T. D. Cohen, in *From Fields to Strings*, edited by M. Shifman *et al.* (World Scientific, Singapore, 2005), Vol. 1, pp. 101–120.
[12] L. McLerran and R. D. Pisarski, Nucl. Phys. **A796**, 83 (2007).
[13] G. Aarts, E. Seiler, and I.-O. Stamatescu, Phys. Rev. D **81**, 054508 (2010); G. Aarts and F. A. James, J. High Energy Phys. 01 (2012), 118.
[14] S. Necco and R. Sommer, Nucl. Phys. **B622**, 328 (2002).
[15] P. de Forcrand *et al.*, Proc. Sci., LATTICE 2011 (2011), 212; (private communication).
[16] S. Hands, S. Kim, and J.-I. Skullerud, Phys. Rev. D **81**, 091502 (2010).